Small target compatible dimensional and analytical metrology for semiconductor nanostructures using X-ray fluorescence techniques

Philipp Hönicke[a], Yves Kayser[a], Victor Soltwisch[a], Andre Wählisch[a], Nils Wauschkuhn[a], Jeroen E. Scheerder[b], Claudia Fleischmann[b,c], Janusz Bogdanowicz[b], Thomas Siefke[d], Anna Andrle[a], Grzegorz Gwalt[e], Frank Siewert[e], Richard Ciesielski[a], and Burkhard Beckhoff[a]

[a]Physikalisch-Technische Bundesanstalt, Abbestr. 2-12, 10587 Berlin, Germany
[b]imec, Kapeldreef 75, Leuven, 3001 Belgium
[c]KU Leuven, Celestijnenlaan 200D, Leuven, 3001 Belgium
[d]Friedrich-Schiller-Univ. Jena, Max-Wien-Platz 1, 07745 Jena, Germany
[e]Helmholtz-Zentrum Berlin für Materialien und Energie GmbH, Albert-Einstein-Str. 15, 12489 Berlin, Germany

ABSTRACT

X-ray fluorescence techniques in special operation modes can provide valuable quantitative insights for semiconductor related applications and can be made compatible to typical sizes of homogenously structured metrology pads. As they are usually in the order to several 10 μm per direction, it must be ensured that no adjacent regions are irradiated or that no X-ray fluorescence from adjacent areas reaches the detector. As this can be realized by using small excitation beams, a multitude of information can e retrieved from such XRF data. In addition to elemental composition, including sensitivity to sub-surface features on can derive quantitative amounts of material and even dimensional properties of the nanostructures under study. Here, we show three different approaches for studies related to semiconductor applications that are capable to be performed on real world dies with commonly sized metrology pads.

Keywords: Manuscript format, template, SPIE Proceedings, LaTeX

1. INTRODUCTION

The technological advances in the field of nanoelectronics, especially for lithography[1] as well as the ongoing pursuit of Moore's law[2] result in a drastically increased complexity of the three dimensional structure of a modern semiconductor device. The reasons are on the one hand side the incorporation of many different materials[3] and on the other hand, the decreasing critical feature dimensions[4–6] as well as the growing importance of the third dimension for a further densification of the structures.[7,8] It is easy to imagine that these developments require a significant amount of metrology in order to be producible at a reasonable yield.[4,9,10]

Therefore, 3D-metrology plays a crucial role for these developments as well as for the quality control during manufacturing. Typical metrology techniques being used in this context are electron microscopy based techniques, either scanning electron microscopy (SEM) or transmission electron microscopy (TEM), which reveal topographical details with high spatial resolution but no elemental sensitivity if not coupled with an energy-dispersive X-ray (EDX) instrument. However, existing metrology options are approaching inherent limits. For example, sub-surface or buried nanoobjects such as a lateral cavity etch[11] are either inaccessible to techniques such as scanning electron microscopy or can be made accessible only very localized (e.g., using cross-sectional transmission electron microscopy).

X-ray fluorescence based techniques can help to overcome these limitations due to the superior penetration behaviour of X-rays. It is a non-destructive technique and provides an elemental discrimination capability and

Further author information: (Send correspondence to P.H.)
P.H.: E-mail: philipp.hoenicke@ptb.de

thus allows to probe the elemental composition of the sample. Employing grazing incidence XRF, 2D and 3D nanostructures can also be characterized with respect to their dimensional parameters.[12–14] However, typical XRF techniques are not directly compatible to typical metrology pad sizes, which are in the order of a few hundred μm^2 or smaller. Especially if grazing incident techniques are to be used, the beam footprint on the sample surface is much larger resulting in cross-talk signals from surrounding areas.

In this work, several recent XRF-related developments of the Physikalisch-Technische Bundesanstalt for semiconductor related scientific questions will be presented. On the one hand side, μXRF is employed to study elemental compositions with lateral resolution in the order of 10 μm. By adopting the reference-free XRF approach,[15] absolute quantification of elemental mass depositions can be performed. Employing an X-ray microscope with a more sophisticated focussing unit, even smaller lateral resolution in the order of 100 nm can be achieved allowing also for absolute quantification of amounts of material at such lateral resolution.[16] In fact, this technique even allows to count the atoms within individual nanoobjects and to reconstruct dimensional properties of these objects. Furthermore, we enabled a dimensional and compositional reconstruction of arrays of nanostructures on small targets by grazing exit XRF.[17] This technique provides sub-nm sensitivity for dimensional properties of the nanostructure in addition to the compositional information. All of these techniques are readily compatible to typical target sizes.

Even though we are using synchrotron radiation beamlines as excitation sources, the presented techniques either are already available by commercial vendors or can in principle be made available on laboratory scale instruments.

2. REFERENCE-FREE μXRF

The so-called μXRF technique is based on mapping the sample using a micrometer sized incident beam recording the emitted X-ray fluorescence radiation from the sample at each position. Such experiments can be realized employing capillary optics to focus the beam into a small spot. Even though several commercial vendors for such instruments exist, it is not yet a common technique in semiconductor related metrology. But for next generation device structures, μXRF is being studied to probe sub-surface features such as cavities.[11,18]

In many cases however, a quantitative information about the compositional changes versus sample position is needed and simple fluorescence count rate distributions are not sufficient. Existing fundamental parameter (FP) based physical quantification schemes for μ-XRF,[19,20] however, require a pre-calibration of the employed instrument using adequate calibration samples as well as a good knowledge of the transmission behaviour of the employed micro focusing optic.

Here, we present a reference-free μ-XRF approach, which allows to derive absolute quantitative information from the recorded elemental maps without the need for any calibration. Employing physically calibrated instrumentation, the emitted fluorescence intensities from the sample can be recorded and the elemental mass depositions of the elements of interest can be calculated. Using a monocapillary optic, beam focus sizes in the order of 15 μm full-width-at-half-maximum (FWHM) can easily be achieved. A sketch of the setup employed is shown in part a of figure 1.

We have applied this setup to study the SiGe recess etch in so-called fork-sheet nanostructures[21] from imec. Here, the SiGe serves as sacrifical material that is to be removed during recess etching. In figure 1 b) a TEM cross section of the nanostructure before etch (A) is shown with the SiGe as the white part. For two different recess etch durations (B and C), the removal of the SiGe progresses. Regular gratings of these structures are available on the die in 80 μm by 80 μm large pads as indicated in the picture as the region of interest (ROI).

This ROI as well as surrounding areas were mapped for several dies of each etch state. Fluorescence intensity maps (part d of figure 1) can be derived and the ROI area can be easily localized (part c). Here, an averaged emitted fluorescence intensity for each element of interest can be derived within the marked region (horizontal and vertical dashed lines) in order to derive the present mass deposition of germanium, oxygen and nitrogen (not shown). These can either be compared directly (part f of figure 1) employing the standard deviation within the averaged area or further processed to derive the number of remaining Ge atoms per unit area. Using the information about the SiGe stoichiometry and its density[22] and the geometrical information about the nanostructure, also a total SiGe thickness can be calculated (part e). Here, we clearly found remaining Ge n the nominally fully etched wafer (C) which corresponds to about 3 % of the originally present Ge.

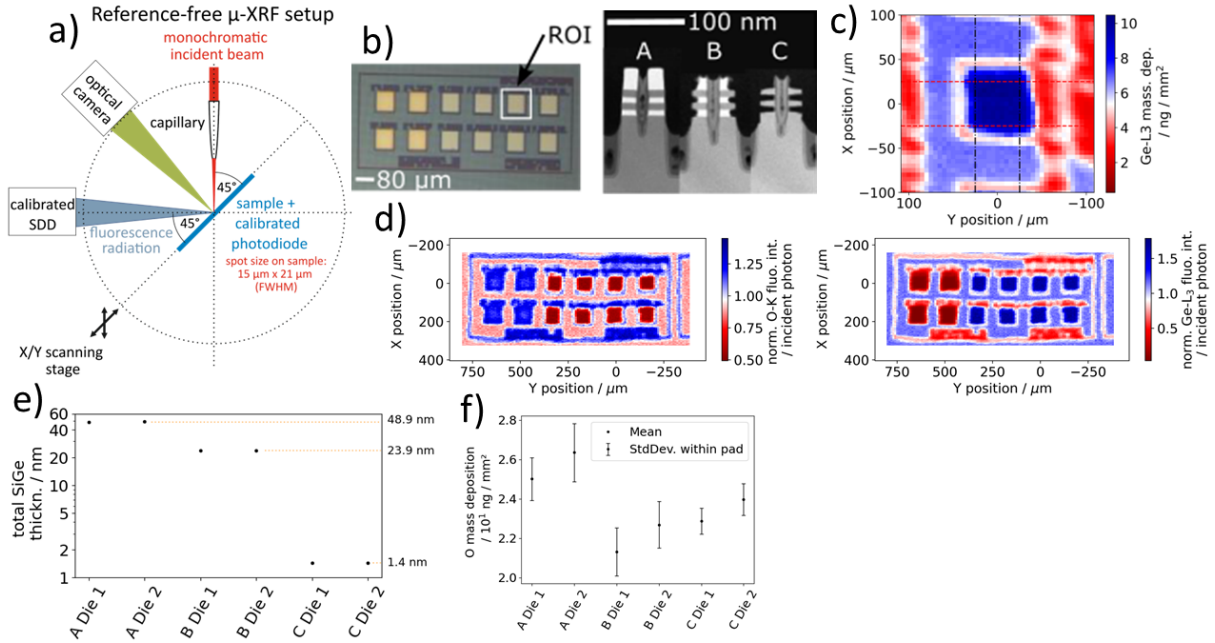

Figure 1. a) schematic view of the experimental arrangement for reference-free μXRF, b) images of the target area and cross section of the available fork sheet nanostructures, c) focussed map of the measured Ge mass deposition in the vicinity of the indicated region of interest (ROI), d) full area maps for oxgen and germanium fluorescence intensities, e) quantified remaining SiGe thickness equivalent within the forks, f) quantified oxygen mass deposition within the ROI

3. REFERENCE-FREE NM-XRF

Very similar experiments can be performed employing our setup for X-ray microscopy (XRM).[16,23] Here, we adopt a rather simple optical bench consisting of a pinhole, a fresnel zone plate and an order selection apperture (OSA) to enable XRM experiments at the PGM beamline.[24] The set-up is mounted on a 6-axis manipulator[25] which allows for an alignment of all three linear as well as all three rotational axes. The optics and the transmission sample are mounted on piezo positioning stages with 8 axes providing 1 nm resolution and encoder control. A sketch of the setup is shown in fugure 2 part a.Even though the achievable spatial resolution, which is in the 100 nm regime, is not competitive to dedicated XRM setups, this instrument can provide interesting insights as it is suited to derive quantitative information.

Similarly as for the μ-XRF approach, absolute amounts of material can be derived from the measured fluorescence mappings by performing reference-free quantification.[16] But more importantly, the number of atoms within a nanostructure can be quantified within certain limitations employing a reconstruction of the measurement process.[16] During this reconstruction, the 3d elemental composition and dimensions are convolved with a model of the incident beam. The resulting fluorescence intensity of the element of interest is calculated and matched against the experimental data to derive a representative set of model parameters.

In parts c and d of figure 3 the resulting model data for two different nanoobjects is shown in comparison to the experimental data. From this reconstructed 3d model of the nanoobject, the varous dimensional parameters can be compared and validated against other techniques available (see part b of figure 3). Here, the agreement with respect to the derived width and height is quite well. The deviation on the derived length as well as the relatively large uncertainties could be further reduced by increasing the point density during the mapping. Further details about this technique can be found in ref.[16]

4. GRAZING EXIT XRF

With an experimental technique called grazing-exit X-ray fluorescence, we can provide similar results for an ensemble of regularly ordered nanoobjects[17] and not for single nanoobjects. The technique is based on exciting

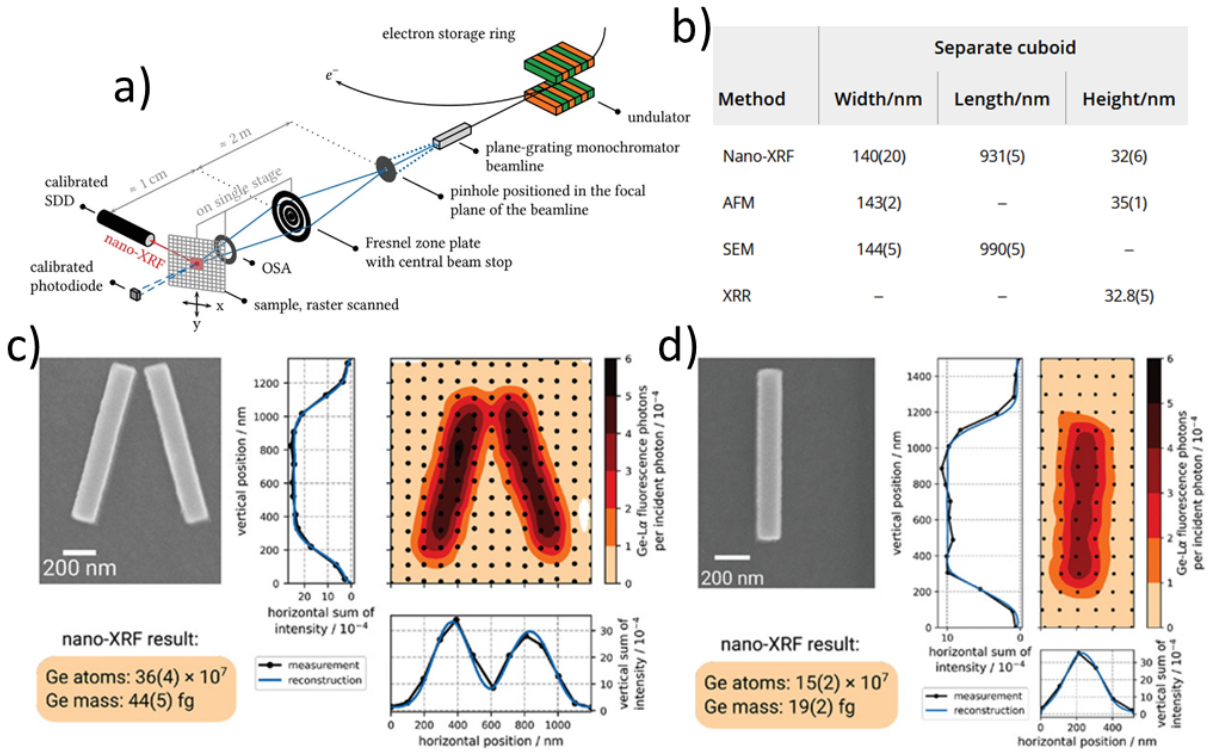

Method	Separate cuboid		
	Width/nm	Length/nm	Height/nm
Nano-XRF	140(20)	931(5)	32(6)
AFM	143(2)	–	35(1)
SEM	144(5)	990(5)	–
XRR	–	–	32.8(5)

Figure 2. a) schematic view of the experimental set-up for nm-XRF, b) reconstructed dimensional properties for cuboid nanostructure (shown in d), c) SEM image, experimental data and reconstruction result of tilted cuboids, d) SEM image, experimental data and reconstruction result of isolated cuboid

X-ray fluorescence radiation in the area of interest and detecting it using a position and photon energy sensitive detector such as a CCD camera (part a of figure 3). If that detector is aligned well with the orientation of the nanostructures very distinct fluorescence intensity patterns can be recorded (see part b of figure 3). This examplary dataset is from a TiO_2 capped silicon fin structure as sketched in part d of figure 3 and shows both the experimentally recorded Ti fluorescence intensity map (left side) and a simulated map (right side) for a reconstruction of the nanostructure.

The reconstruction is based on a parameterized model of the nanostructure cross section as shown in the left part of figure 3 d. The optimal parameters are determined by performing finite element solver based calculations for the X-ray standing wave forming inside and around the nanostructure at each exit angle pair. By matching the experimental data with the calculation the nanostructures parameters are reconstructed. Comparison with AFM and TEM reveals a high degree of agreement (parts c and d of figure 3).

This type of experiment if easily applicable to small target sizes due to the relatively high incident angles needed for excitation. As demonstration examples an array of vertical SiGe nanowire structures[26] (inset e) and an array of fork sheet transistor structures (inset f) was measured using the GEXRF technique. For both examples, the obtained Ge-Ka fluorescence intensity distributions are very rich in angular variations from which the dimensional properties of the nanostructures could be reconstructed. Further details about this technique can be found in ref.[17]

5. CONCLUSIONS

In the present work we demonstrate our toolset for X-ray fluorescence based characterization techniques for state-of-the-art nanostructures for semiconductor applications. All of these techniques are compatible to typical test pad sizes and can be applied to look at lateral distributions for a wide range of chemical elements in a quantitative manner. Due to the superior penetration characteristics of X-rays, also buried parts of such nanostructures can

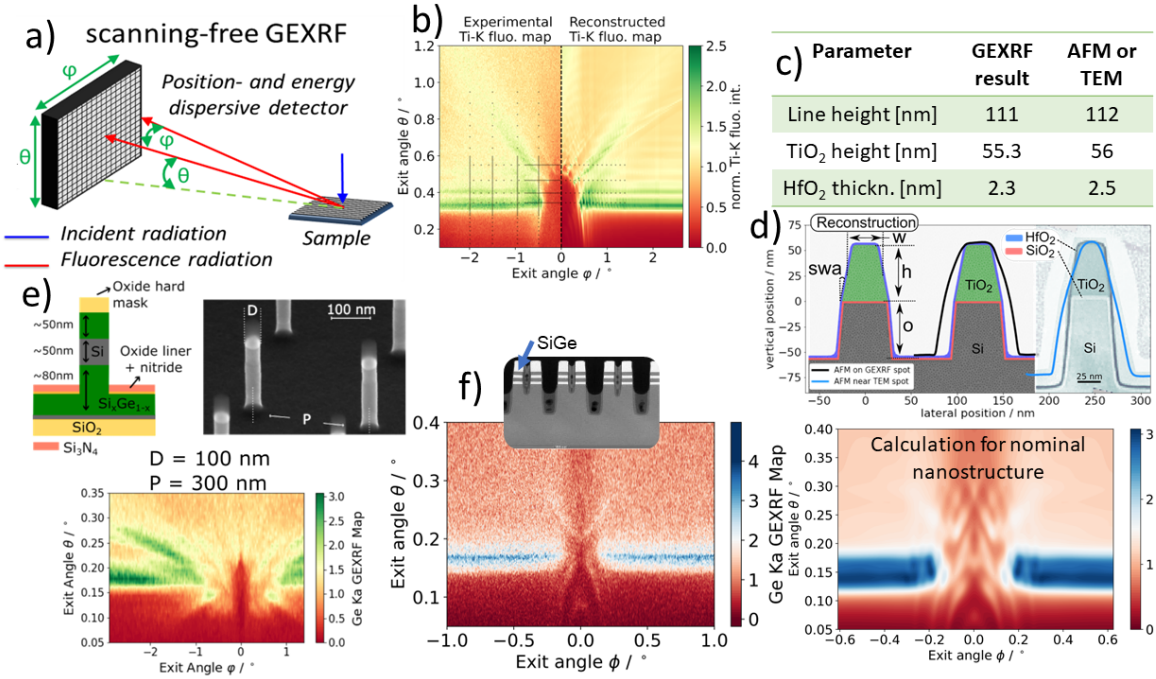

Figure 3. a) schematic view of the experimental arrangement, b) comparison of an experimental GEXRF map (lft) versus a reconstructed map (right) for the nanostructure shown in d, c) reconstruction results in comparison to TEM and AFM data, d) parameterization, cross section and comparison to TEM and AFM of GEXRF reconstructed nanostructure, e) SiGe nanowire structures and a recorded Ge fluorescence map, f) Fork Sheet nanostructures with SiGe layers, an experimental Ge fluorescence map and a calculation based on the nominal nanostructure parameters

easily be characterized. Employing the nm-XRF and GEXRF techniques, also dimensional properties of the nanostructures can be reconstructed with sensitivities in the low nm regime or even below. A more detailed overview about these two techniques is provided in dedicated works.[16,17]

ACKNOWLEDGMENTS

This project has received funding from the ECSEL Joint Undertaking (JU) under grant agreement No 875999-IT2 and No. 826589-MADEin4. The JU receives support from the European Union's Horizon 2020 research and innovation programme and the Netherlands, Belgium, Germany, France, Austria, Hungary, the United Kingdom, Romania and Israel.

REFERENCES

[1] Wagner, C. and Harned, N., "Lithography gets extreme," *Nature Photonics* **4**, 24–26 (jan 2010).
[2] Moore, G., "Cramming more components onto integrated circuits," *Electronics* **38(8)**, 114–117 (1965).
[3] Clark, R., "Emerging applications for high k materials in vlsi technology," *Materials* **7**, 2913–2944 (2014).
[4] King, S., Simka, H., Herr, D., Akinaga, H., and Garner, M., "Research updates: The three m's (materials, metrology, and modeling) together pave the path to future nanoelectronic technologies," *APL Materials* **1**, 040701 (2013).
[5] Natarajan, S., Agostinelli, M., Akbar, S., Bost, M., Bowonder, A., Chikarmane, V., Chouksey, S., Dasgupta, A., Fischer, K., Fu, Q., Ghani, T., Giles, M., S. Govindaraju, R. G., Han, W., Hanken, D., Haralson, E., Haran, M., Heckscher, M., Heussner, R., Jain, P., James, R., Jhaveri, R., Jin, I., Kam, H., Karl, E., Kenyon, C., Liu, M., Luo, Y., Mehandru, R., Morarka, S., Neiberg, L., Packan, P., Paliwal, A., Parker, C., Patel, P., Patel, R., Pelto, C., Pipes, L., Plekhanov, P., Prince, M., Rajamani, S., Sandford, J., Sell, B., Sivakumar, S., Smith, P., Song, B., Tone, K., Troeger, T., Wiedemer, J., Yang, M., and Zhang, K., "A 14nm logic

technology featuring 2nd-generation finfet, air-gapped interconnects, self-aligned double patterning and a 0.0588 μm^2 sram cell size," *Electron Devices Meeting (IEDM), 2014 IEEE International* , 3.7.1 – 3.7.3 (2014).

[6] Kim, R. R.-H., Sherazi, S. M. Y., Debacker, P., Raghavan, P., Ryckaert, J., Malik, A., Verkest, D., Lee, J. U., Gillijns, W., Tan, L. E., Blanco, V., Ronse, K., and McIntyre, G., "IMEC n7, n5 and beyond: DTCO, STCO and EUV insertion strategy to maintain affordable scaling trend," *Design-Process-Technology Co-optimization for Manufacturability XII* (mar 2018).

[7] Vandooren, A., Franco, J., Wu, Z., Parvais, B., Li, W., Witters, L., Walke, A., Peng, L., Deshpande, V., Rassoul, N., Hellings, G., Jamieson, G., Inoue, F., Devriendt, K., Teugels, L., Heylen, N., Vecchio, E., Zheng, T., Rosseel, E., Vanherle, W., Hikavyy, A., Mannaert, G., Chan, B. T., Ritzenthaler, R., Mitard, J., Ragnarsson, L., Waldron, N., Heyn, V. D., Demuynck, S., Boemmels, J., Mocuta, D., Ryckaert, J., and Collaert, N., "First demonstration of 3d stacked finfets at a 45nm fin pitch and 110nm gate pitch technology on 300mm wafers," *2018 IEEE International Electron Devices Meeting (IEDM)* (dec 2018).

[8] Ryckaert, J., Schuddinck, P., Weckx, P., Bouche, G., Vincent, B., Smith, J., Sherazi, Y., Mallik, A., Mertens, H., Demuynck, S., Bao, T. H., Veloso, A., Horiguchi, N., Mocuta, A., Mocuta, D., and Boemmels, J., "The complementary FET (CFET) for CMOS scaling beyond n3," *2018 IEEE Symposium on VLSI Technology* (jun 2018).

[9] Bunday, B., "Hvm metrology challenges towards the 5 nm node," *Proc. of SPIE* **9778**, 97780E (2016).

[10] Bunday, B., Solecky, E., Vaid, A., Bello, A., and Dai, X., "Metrology capabilities and needs for 7nm and 5nm logic nodes," *Proc. SPIE 10145* (Metrology, Inspection, and Process Control for Microlithography XXXI), 101450G (2017).

[11] Bogdanowicz, J., Oniki, Y., Kenis, K., Muraki, Y., Nuytten, T., Sergeant, S., Franquet, A., Spampinato, V., Conard, T., Hoflijk, I., Meersschaut, J., Claessens, N., Moussa, A., den Heuvel, D. V., Hung, J., Koret, R., Charley, A.-L., and Leray, P., "Spectroscopy: a new route towards critical-dimension metrology of the cavity etch of nanosheet transistors," *Metrology, Inspection, and Process Control for Semiconductor Manufacturing XXXV* (feb 2021).

[12] Soltwisch, V., Hönicke, P., Kayser, Y., Eilbracht, J., Probst, J., Scholze, F., and Beckhoff, B., "Element sensitive reconstruction of nanostructured surfaces with finite-elements and grazing incidence soft x-ray fluorescence," *Nanoscale* **10**, 6177–6185 (2018).

[13] Nikolaev, K. V., Soltwisch, V., Hönicke, P., Scholze, F., de la Rie, J., Yakunin, S. N., Makhotkin, I. A., van de Kruijs, R. W. E., and Bijkerk, F., "A semi-analytical approach for the characterization of ordered 3d nanostructures using grazing-incidence x-ray fluorescence," *Journal of Synchrotron Radiation* **27**, 386–395 (feb 2020).

[14] Hönicke, P., Andrle, A., Kayser, Y., Nikolaev, K. V., Probst, J., Scholze, F., Soltwisch, V., Weimann, T., and Beckhoff, B., "Grazing incidence-x-ray fluorescence for a dimensional and compositional characterization of well-ordered 2d and 3d nanostructures," *Nanotechnology* **31**, 505709 (oct 2020).

[15] Beckhoff, B., "Traceable characterization of nanomaterials by x-ray spectrometry using calibrated instrumentation," *Nanomaterials* **12**, 2255 (jun 2022).

[16] Wählisch, A., Unterumsberger, R., Hönicke, P., Lubeck, J., Kayser, Y., Weser, J., Dai, G., Hahm, K., Weimann, T., Seim, C., Rehbein, S., and Beckhoff, B., "Quantitative element-sensitive analysis of individual nanoobjects," *Small* , 2204943 (dec 2022).

[17] Hönicke, P., Kayser, Y., Nikolaev, K. V., Soltwisch, V., Scheerder, J. E., Fleischmann, C., Siefke, T., Andrle, A., Gwalt, G., Siewert, F., Davis, J., Huth, M., Veloso, A., Loo, R., Skroblin, D., Steinert, M., Undisz, A., Rettenmayr, M., and Beckhoff, B., "Simultaneous dimensional and analytical characterization of ordered nanostructures," *Small* **18**, 2105776 (nov 2021).

[18] Breton, M. A., Schmidt, D., Greene, A., Frougier, J., and Felix, N., "Review of nanosheet metrology opportunities for technology readiness," *Journal of Micro/Nanopatterning, Materials, and Metrology* **21** (apr 2022).

[19] Kanngießer, B., "Quantification procedures in micro x-ray fluorescence analysis," *Spectrochimica Acta Part B: Atomic Spectroscopy* **58**, 609–614 (apr 2003).

[20] Mantouvalou, I., Malzer, W., and Kanngießer, B., "Quantification for 3d micro x-ray fluorescence," *Spectrochimica Acta Part B: Atomic Spectroscopy* **77**, 9–18 (nov 2012).

[21] Weckx, P., Ryckaert, J., Litta, E. D., Yakimets, D., Matagne, P., Schuddinck, P., Jang, D., Chehab, B., Baert, R., Gupta, M., Oniki, Y., Ragnarsson, L.-A., Horiguchi, N., Spessot, A., and Verkest, D., "Novel forksheet device architecture as ultimate logic scaling device towards 2nm," *2019 IEEE International Electron Devices Meeting (IEDM)* (dec 2019).

[22] Levinshtein, M. E., Rumyantsev, S. L., and Shur, M. S., [*Properties of Advanced Semiconductor Materials: GaN, AIN, InN, BN, SiC, SiGe*], John Wiley & Sons (2001).

[23] Lubeck, J., Seim, C., Dehlinger, A., Haidl, A., Hönicke, P., Kayser, Y., Unterumsberger, R., Fleischmann, C., and Beckhoff, B., "A compact vibration reduced set-up for scanning nm-XRF and STXM.," *Microscopy and Microanalysis* **24**, 162–163 (aug 2018).

[24] Senf, F., Flechsig, U., Eggenstein, F., Gudat, W., Klein, R., Rabus, H., and Ulm, G., "A plane-grating monochromator beamline for the ptb undulators at BESSY II," *J. Synchrotron Rad.* **5**, 780–782 (1998).

[25] Lubeck, J., Beckhoff, B., Fliegauf, R., Holfelder, I., Hönicke, P., Müller, M., Pollakowski, B., Reinhardt, F., and Weser, J., "A novel instrument for quantitative nanoanalytics involving complementary x-ray methodologies," *Rev. Sci. Instrum.* **84**, 045106 (2013).

[26] Veloso, A., Huynh-Bao, T., Matagne, P., Jang, D., Eneman, G., Horiguchi, N., and Ryckaert, J., "Nanowire and nanosheet fets for ultra-scaled, high-density logic and memory applications," *Solid-State Electron.* **168**, 107736 (jun 2020).